Spin-orbit torque opposing the Oersted torque in ultrathin Co/Pt bilayers

T. D. Skinner, M. Wang, A. T. Hindmarch, A. W. Rushforth, A. C. Irvine, D. Heiss, H. Kurebayashi, and A. J. Ferguson

Citation: Applied Physics Letters **104**, 062401 (2014); doi: 10.1063/1.4864399
View online: http://dx.doi.org/10.1063/1.4864399
View Table of Contents: http://scitation.aip.org/content/aip/journal/apl/104/6?ver=pdfcov
Published by the AIP Publishing

Spin-orbit torque opposing the Oersted torque in ultrathin Co/Pt bilayers

T. D. Skinner,[1,a)] M. Wang,[2] A. T. Hindmarch,[2,b)] A. W. Rushforth,[2] A. C. Irvine,[1] D. Heiss,[1,c)] H. Kurebayashi,[1,d)] and A. J. Ferguson[1,e)]
[1]*Cavendish Laboratory, University of Cambridge, Cambridge CB3 0HE, United Kingdom*
[2]*School of Physics and Astronomy, University of Nottingham, Nottingham NG7 2RD, United Kingdom*

(Received 9 December 2013; accepted 24 January 2014; published online 10 February 2014)

Current-induced torques in ultrathin Co/Pt bilayers were investigated using an electrically driven ferromagnetic resonance technique. The angle dependence of the resonances, detected by a rectification effect as a voltage, was analysed to determine the symmetries and relative magnitudes of the spin-orbit torques. Both anti-damping (Slonczewski) and field-like torques were observed. As the ferromagnet thickness was reduced from 3 to 1 nm, the sign of the sum of the field-like torque and Oersted torque reversed. This observation is consistent with the emergence of a Rashba spin orbit torque in ultra-thin bilayers. © *2014 AIP Publishing LLC*. [http://dx.doi.org/10.1063/1.4864399]

Current-induced spin-orbit torques in ultrathin ferromagnetic/heavy metal bilayers provide ways to electrically control magnetisation. Two mechanisms for observed torques have been proposed, both of which could contribute to the total torques and both of which originate in the spin-orbit interaction. A schematic of both mechanisms is shown in Figure 1(a). The first mechanism is due to the spin-Hall effect (SHE),[1–4] where a charge-current in the heavy metal layer generates spin currents perpendicular to the charge-current. When a spin-current flows into the ferromagnetic layer, it can exert a spin-transfer torque (STT).[5–7] This torque normally follows the anti-damping form predicted by Slonczewski[8] and Berger,[9] but it is known that a field-like non-adiabatic spin transfer torque can also exist.[10–12]

The second mechanism is a "Rashba" spin-orbit torque. Due to the structural inversion asymmetry of the two dissimilar materials at the interface, when a current is applied, the spin-orbit Hamiltonian breaks the degeneracy of the electron spin states near the interface, creating a non-equilibrium spin-accumulation. The electron spins in the ferromagnet, through exchange coupling, can then exert a torque on the magnetic moments. This was initially predicted to give a field-like torque, acting perpendicularly to the interface normal and injected current,[13–15] which was later confirmed by experiments in ultrathin Pt/Co/AlO_x[16–18] and Ta/CoFeB/MgO[19] trilayers. However, further measurements in these layers have confirmed the presence of an additional anti-damping torque.[20,21] A recent experiment, in a single-layer ferromagnet with broken symmetry, has shown that this anti-damping torque can be explained by the precession of the spins, initially polarised along the magnetisation, around the additional current-induced spin-orbit fields.[22] These additional torques have also been modelled theoretically in metal bilayer systems.[23,24]

The torques are further complicated by the additional Oersted torque in the ferromagnetic layer, due to the total current in the heavy metal, which has the same symmetry as the field-like torque. The total torques can be formulated as

$$\boldsymbol{\tau} = \tau_{AD}\hat{\mathbf{m}} \times \hat{\mathbf{y}} \times \hat{\mathbf{m}} - (\tau_F + \tau_{Oe})\hat{\mathbf{y}} \times \hat{\mathbf{m}}, \qquad (1)$$

where the anti-damping (τ_{AD}) and field-like (τ_F) torques can have contributions from both the spin-Hall and Rashba effects. Previous studies have tried to disentangle these two effects by studying the dependence of the torques on the

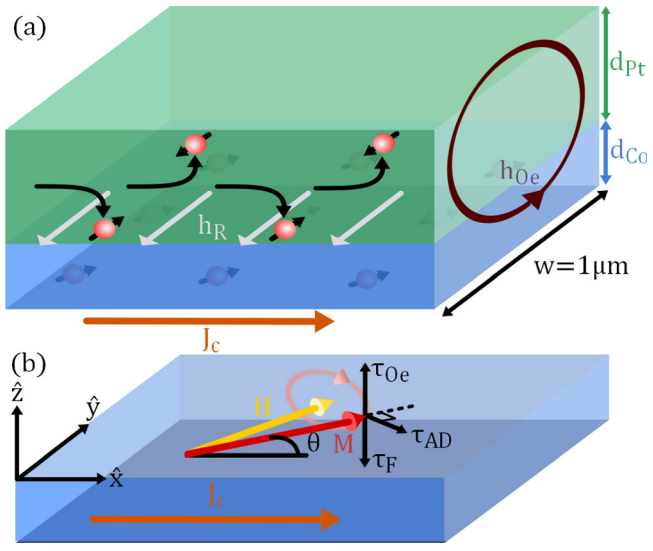

FIG. 1. (a) A charge current density, J_C, passing through the bilayer induces a transverse spin-current in the platinum due to the spin-Hall effect which flows into the cobalt layer. At the interface, due to the structural inversion asymmetry, the conduction electrons experience an effective magnetic field, h_R. The cobalt has an additional oxidised silicon interface which could also similarly produce an effective magnetic field. The current passing through the platinum also induces an Oersted field in the cobalt, due to Ampère's law.(b) The Oersted field induces an out of plane torque on the cobalt magnetisation, τ_{Oe}. Additional anti-damping and field-like torques, τ_{AD} and τ_F, respectively, are induced due to the exchange interaction of the non-equilibrium spin-density in the ferromagnet with the magnetisation. A field-like torque with negative coefficient is shown here opposing a positive Oersted torque.

[a)]Electronic mail: tds32@cam.ac.uk
[b)]Current address: Centre for Materials Physics, Durham University, Durham DH1 3LE, United Kingdom.
[c)]Current address: COBRA Research Institute, Eindhoven University of Technology, Postbus 513, 5600 MB Eindhoven, The Netherlands.
[d)]Current address: London Centre for Nanotechnology, University College London, London WC1H 0AH, United Kingdom.
[e)]Electronic mail: ajf1006@cam.ac.uk

thickness of the two layers.[25,26] In particular, Fan *et al.* observed an additional field-like torque in Py/Pt layers with the same direction as the Oersted field.[26] In this paper, we report a similar field-like torque, emerging only in the ultrathin Co layer regime, opposing the Oersted field. This suggests that the field-like torque is sensitive to details of the sample composition and can vary significantly, possibly due to competing mechanisms.

Using electrically driven ferromagnetic resonance (FMR),[5,27] we have studied sputtered ultrathin bilayers of Co/Pt which are in-plane magnetised, where the cobalt thickness, d_{Co}, is varied between 1 and 3 nm, whilst the platinum thickness, $d_{Pt} = 3$ nm, remains constant. A schematic of the magnetisation precession, and the directions of the torques in our measurement is shown in Figure 1(b). First cobalt and then platinum were deposited on a thermally oxidised silicon substrate by dc magnetron sputtering. $1 \times 10\,\mu$m bars were patterned using electron-beam lithography and Ar ion-milling. Each bar was mounted on a low-loss dielectric circuit board. Microwave power was delivered to the board via a semi-rigid coaxial cable. This was connected to a microstrip transmission line on the circuit board which was terminated by a wirebond to one end of the sample. The other end of the sample was connected to ground via another wirebond. An on-board bias-tee,[28] comprising of an in-line gap capacitor and a wirebond as an inductor, was used to separate the injected microwave power from the measurement of the dc voltage, V_{dc}, across the bar (see Figure 2(a)).

The microwave current injected into the bar, $I_0 e^{j\omega t}$, induces effective magnetic fields, $(h_x, h_y, h_z)e^{j\omega t}$, which drive FMR. As the magnetisation precesses, there is an oscillating component of the resistance due to the anisotropic magnetoresistance (AMR) of the sample: $R = R_0 + \Delta R \cos^2\theta$, where θ is the angular separation of the current and magnetisation. At resonance, this rectifies with the driving microwave current to give a peak in V_{dc}. This can be fitted by a combination of symmetric and antisymmetric Lorentzians[27]

$$V_{dc} = V_{sym}\frac{\Delta H^2}{(H-H_0)^2+\Delta H^2} + V_{asy}\frac{(H-H_0)\Delta H}{(H-H_0)^2+\Delta H^2}, \tag{2}$$

where V_{sym} and V_{asy} are given by

$$V_{sym} = V_{mix}A_{yz}h_z \sin 2\theta \tag{3}$$

and

$$V_{asy} = V_{mix}A_{yy}(h_y \cos\theta - h_x \sin\theta)\sin 2\theta. \tag{4}$$

In these expressions, $V_{mix} = \frac{1}{2}I_0\Delta R$, H_0 and ΔH are the resonant field and linewidth, and A_{yz} and A_{yy} are related to the scalar amplitudes of the ac magnetic susceptibility by $A_{ij} = \chi_{ij}/M_S$. Their values are

$$A_{yz} = \frac{\sqrt{H_0(H_0+M_{eff})}}{\Delta H(2H_0+M_{eff})} \tag{5}$$

and

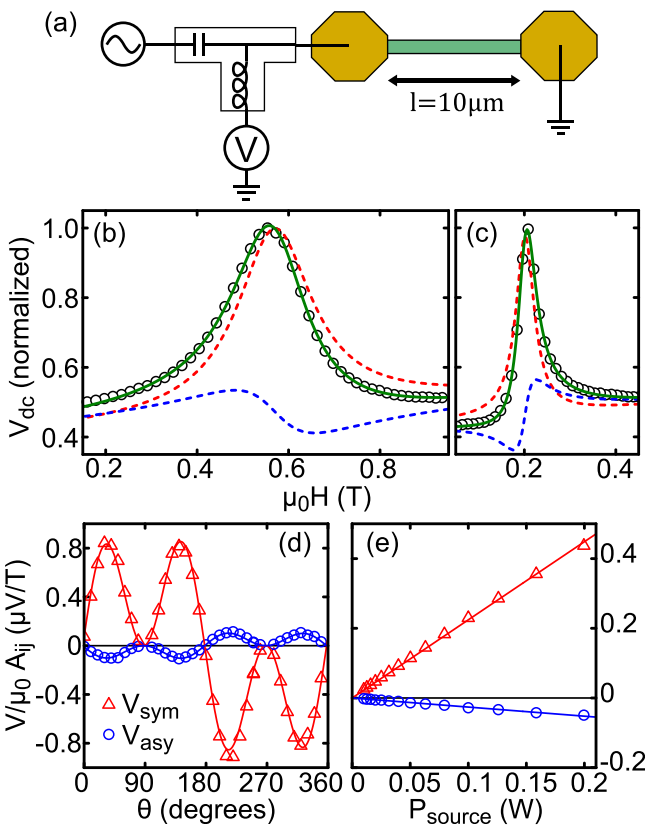

FIG. 2. (a) Schematic of the electrically driven FMR measurement. (b) The resonance in V_{dc} (open circles) for a device with $d_{Co} = 1$ nm, measured with a microwave frequency of 19 GHz, is fitted (solid green line) by a combination of antisymmetric (dashed blue line) and symmetric (dashed red line) Lorentzians. (c) The resonance fitted for a $d_{Co} = 3$ nm device, measured at 16 GHz, shows a reversal in sign of the antisymmetric part compared to $d_{Co} = 1$ nm. (d) The angular dependence of V_{sym}/A_{yz} and V_{asy}/A_{yy} (shown for a device with $d_{Co} = 1.5$ nm) are fitted well by an in-plane anti-damping torque (τ_{AD}) and a combined out of plane Oersted and field-like driving torque ($\tau_{Oe} + \tau_F$), respectively. (e) Both voltages peaks observed scale linearly with the microwave source power, as expected from the theoretically linear dependence on current of the spin-Hall and Rashba effects.

$$A_{yy} = \frac{(H_0+M_{eff})}{\Delta H(2H_0+M_{eff})}. \tag{6}$$

M_{eff} is the effective magnetisation which contains a uniaxial interface anisotropy term

$$M_{eff} = M_S - \frac{H_U^{int}}{d_{Co}}, \tag{7}$$

which depends on the thickness of the cobalt layer, d_{Co}. We do not find voltages with a symmetry of $\sin\theta$, indicating a negligible spin pumping signal. This is because the rectifying microwave current is much larger than the direct current induced via the inverse SHE acting on spin current pumped by the induced precession.

Source microwave powers of 20 dBm were typically used to excite FMR. Microwave frequencies of between 16 and 19 GHz were used to ensure that the entire resonance peak was measured in a magnetic field large enough that the magnetisation was saturated. With microwave power applied, the resonances were measured in V_{dc} as the external magnetic field, H, was swept from high to low at an in-plane angle, θ.

The resonances were measured for successive values of θ, with the peaks then fitted by Eq. (2) (Figures 2(b) and 2(c)). By measuring FMR out of plane and self-consistently fitting the Kittel and energy equations, values of M_{eff} were determined.[29] The fitted values of $\mu_0 M_{\text{eff}}$ were similar to those we have previously reported in spin-pumping measurements of the same layers at 250 K,[30] in this case varying from 1.4 to 0.14 T as d_{Co} is reduced, consistent with Eq. (7). To analyse the data, A_{yz} and A_{yy} are calculated from Eqs. (5) and (6) using the measured values of M_{eff}.

For all the sweeps measured, the symmetric part dominates the antisymmetric part. We now fit the effective fields to $V_{\text{sym}}/A_{\text{yz}}$ and $V_{\text{asy}}/A_{\text{yy}}$ (Figure 2(d)). We find empirically that the symmetric angular dependence can be almost entirely fitted by the anti-damping torque ($h_z \propto \cos\theta$) and that the antisymmetric angular dependence can be almost entirely fitted by a field-like term (h_y independent of angle). Small additional terms which are not consistent in size or sign from device to device are needed for the fitting (h_z independent of angle and $h_y \propto \cos\theta$). These terms are consistent with additional field-like and anti-damping torques with symmetry $\boldsymbol{\tau} \propto \hat{\mathbf{z}} \times \hat{\mathbf{m}}$ and $\boldsymbol{\tau} \propto \hat{\mathbf{m}} \times \hat{z} \times \hat{\mathbf{m}}$, respectively. Most significantly, we see that as the cobalt thickness is reduced from 3 to 1 nm, the sign of the symmetric voltage stays constant, whilst the sign of the antisymmetric voltage flips (see Figures 2(b) and 2(c)). This indicates that as the cobalt thickness is reduced, the sum of the field-like torque and Oersted torque reverses. The voltages measured scale linearly with power (Figure 2(e)), showing the torques are proportional to current density (as V_{mix} is proportional to microwave current).

The microwave currents have previously been directly calibrated in similar measurements using a bolometric technique.[27] In this experiment, we cannot use this technique because of the small temperature coefficient of resistance in the samples. Instead, we compare the relative sizes of the fitted torques induced by the same current. Figure 3 shows the ratio of the Oersted and field-like to anti-damping torques ($(\tau_{\text{F}} + \tau_{\text{Oe}})/\tau_{\text{AD}}$) for the range of cobalt thicknesses measured. We also show the calculated ratio for the case where $\tau_{\text{F}} = 0$ and the anti-damping torque is due to the spin-transfer torque of the spin-Hall spin-current. The calculated ratio is insensitive to the proportion of total current in the platinum layer, as both the Oersted torque and the spin-Hall spin-current originate from the current in the platinum layer. The calculated ratio depends on the values of the spin-Hall angle, θ_{SH}, and the spin-diffusion length, λ_{sf}, of platinum.[5] Here, we have used $\theta_{\text{SH}} = 0.08$ (as reported by Liu *et al.*[5]) for $\lambda_{\text{sf}} = 1, 2$, and 3 nm. For this calculation, we also use saturation magnetisation values, found from SQUID measurements of the layers, of $\mu_0 M_{\text{S}} = 1.45 \pm 0.5$ T (constant in the measured region, $d_{\text{Co}} = 1$ to 2 nm). As the Co layer becomes thicker, we find the ratio converges with the theoretical curve for $\lambda_{\text{sf}} = 1$ nm.[31] However, as d_{Co} reduces below around 2 nm, the ratio become negative and diverges from the theoretical curves, indicating the presence of a field-like torque, τ_{F}, which increasingly opposes the Oersted torque. We note that if we use more conservative values for our theoretical modelling (larger λ_{sf}, smaller θ_{SH}), τ_{F} is even larger.

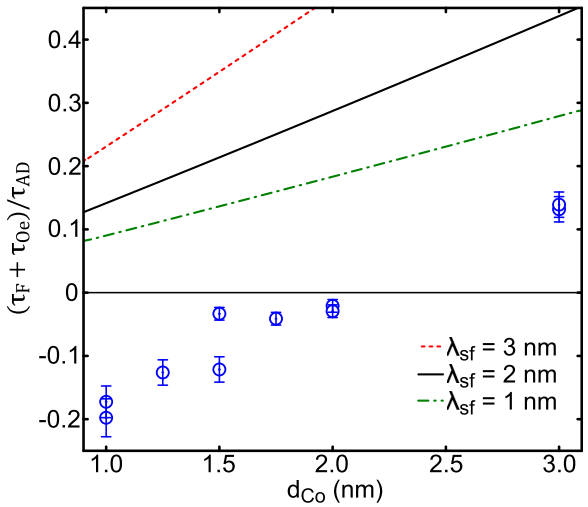

FIG. 3. The ratio of the sum of the Oersted and field-like torque to anti-damping torque is calculated for a series of cobalt thicknesses ($d_{\text{Pt}} = 3$ nm). The error bars show the uncertainty due to the fitting of the torque values to the data. Further scatter in the data may be due to variation within each layer studied. Additionally, we also show the calculated torque ratio for the model presented by Liu *et al.*[5] where only the Oersted torque and the anti-damping torque purely due to the spin-transfer torque of the spin-Hall spin current are considered. We plot the theoretical curves for $\theta_{\text{SH}} = 0.08$ (the same as Liu *et al.* reported for their self-calibration method), for Pt spin-diffusion lengths of 1, 2, and 3 nm.

This reversal in sign of the total field-like torque has not been observed before in Co/Pt. We note that the sign of our τ_{F} and τ_{AD} is consistent with the torques observed by Garello *et al.* at low frequency in an AlOx/Co(0.6 nm)/Pt(3 nm) device.[21] Equally, in the $d_{\text{Co}} = 3$ nm layer, where τ_{F} is weakest, the torques resemble those measured by Liu *et al.* at microwave frequencies in Py(4 nm)/Pt(6 nm)[5] and CoFeB(3 nm)/Pt(6 nm).[6]

Kim *et al.* have studied the torques at low frequency as a function of ferromagnet thickness (0.9 to 1.3 nm) in CoFeB/Ta(1 nm).[25] They observed a constant τ_{AD} with opposite sign because the spin-Hall angle is negative in Ta. τ_{F} increased in the thinner ferromagnet layers, but in contrast to our observation, added to the Oersted torque.

Fan *et al.* have measured the torques at low frequency, with a Cu spacer layer inserted between a Py and Pt layer.[26] A field-like torque was observed even with the spacer layer, and reduced with increasing spacer thickness, indicating that the torque was likely to be a non-adiabatic STT. As the ferromagnet thickness was reduced, the torque increased and added to the Oersted torque. This is the opposite sign to the τ_{F} we have observed in Co/Pt. Fan *et al.* also studied CoFeB/Ta layers using electrically driven FMR. It could be seen that as the thickness of the ferromagnet is reduced, the field-like torque increases, and opposes the Oersted field. This is the opposite sign to the observation of Kim *et al.*

When trying to reconcile these previous measurements with our own, we consider it likely that differing material parameters in each experiment, the quality of the interfaces and the degree of oxidation of the additional ferromagnet interface could give quite different results. Nonetheless, the trend and sign of the field-like torque we observe is consistent with the studies by Liu *et al.* and Garello *et al.* Furthermore,

if the direction of the Rashba field is inverted in CoFeB/Ta compared to Co/Pt,[19] or if the non-adiabatic STT depends on the negative sign of the SHE in Ta, our results can also be consistent with Kim *et al*. and an earlier measurement by Suzuki *et al*.[19] The sign of τ_F we measure opposes the Oersted field and is opposite to the one measured by Fan *et al*. in Py/Pt. This can be explained by the torque we measure having a different origin from Fan *et al*. with Cu spacers strongly indicate a non-adiabatic STT origin in their case. In contrast, our τ_F opposing the Oersted field is consistent with a Rashba field, with opposite sign to the non-adiabatic STT, dominating in our material.

In conclusion, using an electrically driven FMR technique, we have observed an increase in the field-like torque, as a proportion of the total spin-orbit torques, as the cobalt layer is reduced from 3 to 1 nm. This field-like torque opposes the Oersted torque. The enhancement in the torque is consistent with a Rashba field and takes the opposite sign to previous measurements in Py/Pt where the torque was shown to mostly originate non-locally from the interface, in the platinum layer. Whilst this is consistent with a Rashba origin of the field-like torque, we cannot rule out a contribution from a non-adiabatic STT.

A.W.R. acknowledges support from an EPSRC Career Acceleration Fellowship Grant No. EP/H003487/1. A.J.F. acknowledges support from the Hitachi research fellowship and a Royal Society Research Grant (No. RG110616).

[1]J. Hirsch, Phys. Rev. Lett. **83**, 1834 (1999).
[2]J. Sinova, D. Culcer, Q. Niu, N. Sinitsyn, T. Jungwirth, and A. MacDonald, Phys. Rev. Lett. **92**, 126603 (2004).
[3]Y. Kato, R. Myers, A. Gossard, and D. Awschalom, Science **306**, 1910 (2004).
[4]J. Wunderlich, B. Kaestner, J. Sinova, and T. Jungwirth, Phys. Rev. Lett. **94**, 047204 (2005).
[5]L. Liu, T. Moriyama, D. C. Ralph, and R. A. Buhrman, Phys. Rev. Lett. **106**, 036601 (2011).
[6]L. Liu, C.-F. Pai, Y. Li, H. W. Tseng, D. C. Ralph, and R. A. Buhrman, Science **336**, 555 (2012).
[7]L. Liu, O. J. Lee, T. J. Gudmundsen, D. C. Ralph, and R. A. Buhrman, Phys. Rev. Lett. **109**, 096602 (2012).
[8]J. Slonczewski, J. Magn. Magn. Mater. **159**, L1 (1996).
[9]L. Berger, Phys. Rev. B **54**, 9353 (1996).
[10]S. Zhang, P. M. Levy, and A. Fert, Phys. Rev. Lett. **88**, 236601 (2002).
[11]M. A. Zimmler, B. Özyilmaz, W. Chen, A. D. Kent, J. Z. Sun, M. J. Rooks, and R. H. Koch, Phys. Rev. B **70**, 184438 (2004).
[12]J. C. Sankey, Y.-T. Cui, J. Z. Sun, J. C. Slonczewski, R. A. Buhrman, and D. C. Ralph, Nat. Phys. **4**, 67 (2008).
[13]A. Manchon and S. Zhang, Phys. Rev. B **78**, 212405 (2008).
[14]K. Obata and G. Tatara, Phys. Rev. B **77**, 214429 (2008).
[15]A. Manchon and S. Zhang, Phys. Rev. B **79**, 094422 (2009).
[16]I. M. Miron, G. Gaudin, S. Auffret, B. Rodmacq, A. Schuhl, S. Pizzini, J. Vogel, and P. Gambardella, Nature Mater. **9**, 230 (2010).
[17]I. M. Miron, T. Moore, H. Szambolics, L. D. Buda-Prejbeanu, S. Auffret, B. Rodmacq, S. Pizzini, J. Vogel, M. Bonfim, A. Schuhl *et al*., Nature Mater. **10**, 419 (2011).
[18]U. H. Pi, K. Won Kim, J. Y. Bae, S. C. Lee, Y. J. Cho, K. S. Kim, and S. Seo, Appl. Phys. Lett. **97**, 162507 (2010).
[19]T. Suzuki, S. Fukami, N. Ishiwata, M. Yamanouchi, S. Ikeda, N. Kasai, and H. Ohno, Appl. Phys. Lett. **98**, 142505 (2011).
[20]I. M. Miron, K. Garello, G. Gaudin, P.-J. Zermatten, M. V. Costache, S. Auffret, S. Bandiera, B. Rodmacq, A. Schuhl, and P. Gambardella, Nature **476**, 189 (2011).
[21]K. Garello, I. M. Miron, C. O. Avci, F. Freimuth, Y. Mokrousov, S. Blugel, S. Auffret, O. Boulle, G. Gaudin, and P. Gambardella, Nat. Nanotechnol. **8**, 587 (2013).
[22]H. Kurebayashi, J. Sinova, D. Fang, A. Irvine, J. Wunderlich, V. Novak, R. Campion, B. Gallagher, E. Vehstedt, L. Zarbo *et al*., e-print arXiv:1306.1893.
[23]D. A. Pesin and A. H. MacDonald, Phys. Rev. B **86**, 014416 (2012).
[24]X. Wang and A. Manchon, Phys. Rev. Lett. **108**, 117201 (2012).
[25]J. Kim, J. Sinha, M. Hayashi, M. Yamanouchi, S. Fukami, T. Suzuki, S. Mitani, and H. Ohno, Nature Mater. **12**, 240 (2012).
[26]X. Fan, J. Wu, Y. Chen, M. J. Jerry, H. Zhang, and J. Q. Xiao, Nat. Commun. **4**, 1799 (2013).
[27]D. Fang, H. Kurebayashi, J. Wunderlich, K. Vỳbornỳ, L. Zârbo, R. Campion, A. Casiraghi, B. Gallagher, T. Jungwirth, and A. Ferguson, Nat. Nanotechnol. **6**, 413 (2011).
[28]D. Fang, T. Skinner, H. Kurebayashi, R. Campion, B. Gallagher, and A. Ferguson, Appl. Phys. Lett. **101**, 182402 (2012).
[29]K. Ando, S. Takahashi, J. Ieda, Y. Kajiwara, H. Nakayama, T. Yoshino, K. Harii, Y. Fujikawa, M. Matsuo, S. Maekawa, and E. Saitoh, J. Appl. Phys. **109**, 103913 (2011).
[30]T. D. Skinner, H. Kurebayashi, D. Fang, D. Heiss, A. C. Irvine, A. T. Hindmarch, M. Wang, A. W. Rushforth, and A. J. Ferguson, Appl. Phys. Lett. **102**, 072401 (2013).
[31]We note that a value of $\lambda_{sf} = 1$ nm for platinum is much smaller than in most of the literature. However, other studies in bilayers using ferromagnetic magnetic resonance have found similar values, e.g., 1.4 nm in L. Liu, R. A. Buhrman, and D. C. Ralph, e-print arXiv:1111.3702v3 and 1.2 nm in W. Zhang, V. Vlaminck, J. E. Pearson, R. Divan, S. D. Bader, and A. Hoffmann, Appl. Phys. Lett. **103**, 242414 (2013).